Electron- and Positron-Emitting Radiolanthanides for Therapy: Aspects of Dosimetry and Production

Helena Uusijärvi[1], Peter Bernhardt[1], Frank Rösch[2], Helmut R. Maecke[3], and Eva Forssell-Aronsson[1]

[1]Department of Radiation Physics, Göteborg University, Sahlgrenska University Hospital, Göteborg, Sweden; [2]Institute for Nuclear Chemistry, Johannes Gutenberg-University Mainz, Mainz, Germany; and [3]Division of Radiological Chemistry, University Hospital Basel, Basel, Switzerland

All lanthanides have similar chemical properties regarding labeling. Therefore, radiolanthanides that have been used for therapy, such as ^{153}Sm and ^{177}Lu, might easily be replaced with other radiolanthanides. The aim of this work was to investigate the suitability of electron- and positron-emitting radiolanthanides for radionuclide therapy with reference to dosimetry and production possibilities. **Methods:** Radiolanthanides with half-lives of 1 h to 15 d, stable or long-lived daughters, and limited photon emission were selected. The ratio of the absorbed dose rate to the tumors and the normal tissue (*TNḊ*) was calculated for different tumor sizes and compared with the *TNḊ* values for ^{90}Y and ^{131}I. The normal tissue and tumors were simulated as an ellipsoid and spheres, respectively. The *TNḊ* values depend on the physical parameters of the radionuclides, the tumor size, and the ratio between the activity concentrations in the tumor and normal tissue (TNC). **Results:** ^{153}Sm, ^{161}Tb, ^{169}Er, ^{175}Yb, and ^{177}Lu had the highest *TNḊ* values for most of the tumor sizes studied. Among these radiolanthanides, ^{161}Tb and ^{177}Lu are the only ones that can be produced no-carrier-added (*nca*) and with high specific activities. The Auger-electron emitters ^{161}Ho and ^{167}Tm had high *TNḊ* values for tumors weighing less than 1 mg and can be produced *nca* and with high specific activities. ^{142}Pr, ^{145}Pr, and ^{166}Ho showed *TNḊ* values similar to those of ^{90}Y. ^{166}Ho is generator produced and can be obtained *nca* and at high specific activities. ^{143}Pr, ^{149}Pm, ^{150}Eu, ^{159}Gd, ^{165}Dy, ^{176m}Lu, and ^{179}Lu had higher *TNḊ* values than did ^{90}Y for all tumor sizes studied, but only ^{149}Pm can be produced *nca* and at high specific activities. The other electron-emitting radiolanthanides and the positron-emitting radiolanthanides showed low *TNḊ* values for all tumor sizes because of the high photon contribution. **Conclusion:** The low-energy electron emitters ^{161}Tb, ^{177}Lu, and ^{167}Tm might be suitable for radionuclide therapy. The Auger-electron emitter ^{161}Ho might not be suitable for systemic radionuclide therapy (intravenous injection) because of its short half-life but might be suitable for local therapy (e.g., in body cavities). If higher electron energy is needed, ^{149}Pm or ^{166}Ho might be suitable for radionuclide therapy.

Key Words: radiolanthanides; radionuclide therapy; dosimetry; production

J Nucl Med 2006; 47:807–814

Received Oct. 11, 2005; revision accepted Jan. 11, 2006.

For correspondence or reprints contact: Helena Uusijärvi, Department of Radiation Physics, Göteborg University, Sahlgrenska University Hospital, SE-413 45 Göteborg, Sweden.

E-mail: helena.uusijarvi@radfys.gu.se

The 14 elements with atomic numbers between 58 and 71 are called lanthanides. These metal ions all have about the same radius, which makes them chemically similar. Since the beginning of nuclear medicine, radiolanthanides have been considered for use in radionuclide therapy. ^{153}Sm, ^{149}Pm, ^{161}Tb, ^{166}Ho, and ^{177}Lu have been bound to monoclonal antibodies and peptides for treatment of various tumor types (*1*). ^{177}Lu is a low-energy-electron–emitting radiolanthanide that is starting to be used as a replacement for the high-energy-electron–emitting nonlanthanide ^{90}Y. Both ^{90}Y-labeled and ^{177}Lu-labeled somatostatin analogs and antibodies have shown promising results in the treatment of tumors. Promising preclinical results have been obtained with [^{177}Lu-DOTA^{0}, Tyr^{3}]-octreotate (^{177}Lu-DOTATATE) against various neuroendocrine tumors (*1–3*) and with ^{177}Lu-labeled monoclonal antibodies against small peritoneal metastases of colorectal origin (*4*). In the latter study, using a murine model, the median survival time was statistically significantly longer after treatment with ^{177}Lu-MN-14 than with ^{186}Re-MN-14 or ^{90}Y-MN-14 and was longer than with ^{131}I-MN-14 although not statistically significantly so. Encouraging clinical results have also been achieved with ^{177}Lu-DOTATATE and [^{177}Lu-DOTA^{0}-Tyr^{3}]-octreotide (^{177}Lu-DOTATOC) in the treatment of neuroendocrine tumors (*5–9*). Despite the encouraging early therapeutic results with ^{177}Lu in radionuclide therapy, it is not known whether it is the optimal therapeutic radionuclide, and the investigation of other radionuclides for this purpose would thus be valuable. Because all lanthanides have similar chemical properties, they should have similar labeling procedures, and ^{177}Lu might easily be replaced by other radiolanthanides. Furthermore, many other lanthanides also have large cross sections for neutron absorption, and as a result, high activities can often be produced.

As a first criterion for the therapeutic use of radiolanthanides, it is important to study their energy deposition in tumors and in normal tissue. The absorbed dose to normal tissue, and especially to critical organs, needs to be kept as low as possible. Thus, radionuclides with a low photon emission must be used. Photons are useful for diagnostic purposes and biokinetic studies, but normal tissues will be irradiated in an undesired way. Wessels and Rogus

introduced a model for estimation of the influence of photons on the absorbed dose to normal tissue and a single large tumor for therapy with radiolabeled antibodies (*10*). Bernhardt et al. developed this model further to make it valid for different tumor sizes and biodistributions (*11*). They also stressed that this model can be useful even without information about the exact biokinetics (*12*). These models calculate the tumor–to–normal-tissue absorbed dose ratio (TND) and the tumor–to–normal-tissue mean absorbed dose rate ratio ($TN\dot{D}$). These models generate clear parameters for general dosimetric studies of the suitability of different radionuclides for therapy (*11*). In this study, only the $TN\dot{D}$ is calculated because the biodistribution of the labeled substance needs to be known for calculating the TND.

Depending on the production route, either no-carrier-added (*nca*) or carrier-added (*ca*) radionuclides are obtained. High specific activity is necessary for systemic radionuclide therapy (*1,13*), especially when using peptides with pharmacologic side effects (*14*). All electron-emitting radiolanthanides investigated in this study can be produced with nuclear reactors (*15*), either directly or indirectly, or by using accelerators (*1*). A few radiolanthanides can be obtained from radionuclide generator systems (*16*).

The irradiation of stable lanthanide targets at nuclear reactors results in the neutron capture reaction (n,γ). For some targets, double neutron capture is required to produce the desired radioisotope, such as the ^{164}Dy(n,γ)(n,γ)^{166}Dy reaction. The radioactivity batch yield is, in principle, determined according to the equation:

$$A = [h \cdot N] \cdot \sigma \cdot \Phi \cdot (1 - e^{-\lambda t}), \qquad \text{Eq. 1}$$

where h is the fraction of the isotope relevant for neutron capture, N is the atomic number of the lanthanide target, σ is the neutron capture cross section (most relevant is σ_{th}, the probability of absorbing thermal neutrons with energies of approximately 0.025 eV), Φ is the neutron flux, t is the irradiation time, and λ is the decay constant of the produced radioisotope (*1*). Neutron activation induced by epithermal neutrons at energies of between 1 eV and 1 keV may contribute to the radionuclide production yield. In contrast to the production routes discussed here, radiochemical separation of the radiolanthanide from the irradiated target is not possible and the radiolanthanide is *ca*. Nevertheless, because powerful nuclear reactors and isotopically enriched targets are available, this production route is among the more common, in particular if high thermal neutron fluxes of $\Phi_{th} \geq 4 \cdot 10^{14}$ n/cm^2/s are available.

If the neutron capture reaction is followed by a β^- decay of the primary produced nucleus, that is (n,γ) → β^-, then chemical separation is possible, due to the new element formed, and the secondary radionuclide can be obtained *nca*.

Neutron irradiation of nuclei such as ^{233}U induces fission (n, fission), thereby forming a spectrum of radiolanthanides with a maximum yield in the distribution of isotope mass at about 140. These light radiolanthanides may be chemically separated from the uranium target and from the other fission products. They are in *nca* form, but not necessarily isotopically pure, because several radioisotopes are produced for each lanthanide formed in the fission process.

Accelerators principally allow the formation of *nca* radiolanthanides, because the bombardment with accelerated protons, deuterons, and heavier ions results in nuclear processes such as (p,xn), (d,xn), (^{3}He,xn), (α,xn), and many others, yielding products of different proton number. Individual radiolanthanides can be obtained according to the target chosen and the type and energy of the accelerated projectile, but absolute production yields may not reach those of reactor-based production routes.

High-energy proton irradiation results in fragmentation of the target nucleus (p, spallation). A spectrum of *nca* radionuclides is obtained. In addition to off-line radiochemical separation processes, online isotope separation facilities include a mass-separation facility. For the production of radiolanthanides, targets such as tantalum or tungsten are irradiated with protons of, usually, more than 600 MeV.

Several radiolanthanide generators are available, such as ^{134}Ce/^{134}La, ^{140}Nd/^{140}Pr, and ^{166}Dy/^{166}Ho, with the last being the most common. Key advantages of radionuclide generators include the availability of the daughter radionuclide in *nca* form and the convenience of obtaining the desired daughter radionuclide on demand, without having to rely on access to nuclear reactors or accelerators.

The aim of this work was to evaluate the dosimetric and production properties of electron- and positron-emitting radiolanthanides for radionuclide therapy. The investigated radiolanthanides were compared with the nonlanthanide radionuclides ^{90}Y and ^{131}I that are routinely used for clinical therapy today.

MATERIALS AND METHODS

Electron- and positron-emitting radiolanthanides with stable or long-lived daughter nuclides, half-lives between 1 h and 15 d, and low (<5) photon-to-electron (p/e) energy ratios (the sum of the total photon energy emitted per decay divided by the sum of the total electron energy emitted per decay) were selected, together with positron-emitting radiolanthanides proposed for systemic therapy (*1,17,18*). The electron-emitting radiolanthanides, together with their decay data, are given in Table 1, and the positron-emitting radiolanthanides are given in Table 2. The electron emitters ^{134}Ce and ^{140}Nd are listed in Table 2 instead of Table 1, because in practice they represent transient equilibria with their short-lived positron-emitting daughter nuclides ^{134}La and ^{140}Pr.

The $TN\dot{D}$ model was recently developed for general dosimetric evaluation of radionuclides (*11,12*) and is described briefly here. The $TN\dot{D}$ was calculated by a program written in MATLAB 6.5 (The MathWorks Inc.). The whole body was simulated as a 70-kg ellipsoid, with principal axes forming the ratio 1:1.8:9.27, and the tumors were represented by spheres of different sizes. Both the normal tissue and the tumors were assumed to be of unit density matter. The tumor sizes ranged from 1 cell, with a radius of 6.2 μm

TABLE 1
Decay Data for the Electron Emitters Studied (*22,23*)

Element	Radionuclide	Decay mode	Half-life	p/e	Mean β-energy (keV/decay)	Mean electron energy (keV/decay)
Lanthanum	^{140}La	β^-	1.68 d	4.3	525	9
	^{142}La	β^-	1.54 h	3.0	842	—
Praseodymium	^{142}Pr	β^-, EC	19.2 h	0.1	809	—
	^{143}Pr	β^-	13.6 d	9.9×10^{-8}	315	—
	^{145}Pr	β^-	5.98 h	0.02	677	0.4
Promethium	^{149}Pm	β^-	2.21 d	0.03	366	0.7
	^{150}Pm	β^-	2.68 h	1.9	781	11
Samarium	^{153}Sm	β^-	1.95 d	0.2	225	45
Europium	^{150}Eu	β^-, β^+, EC	12.6 h	0.1	299/(e^+ 2)	1
	^{156}Eu	β^-	15.2 d	3.1	395	30
	^{157}Eu	β^-	15.2 h	3.0	372	—
Gadolinium	^{159}Gd	β^-	18.6 h	0.2	305	6
Terbium	^{161}Tb	β^-	6.91 d	0.2	155	42
Dysprosium	^{165}Dy	β^-	2.33 h	0.1	442	7
Holmium	^{161}Ho	EC	2.48 h	1.8	—	32
	^{166}Ho	β^-	1.12 d	0.04	711	29
	^{167}Ho	β^-	3.10 h	1.6	188	42
Erbium	^{169}Er	β^-	9.40 d	5.0×10^{-4}	100	—
Thulium	^{167}Tm	EC	9.24 d	1.2	—	126
	^{172}Tm	β^-	2.65 d	0.9	493	39
	^{173}Tm	β^-	8.24 h	1.3	293	16
Ytterbium	^{175}Yb	β^-	4.19 d	0.3	127	4
Lutetium	^{176m}Lu	β^-	3.64 h	0.03	390	39
	^{177}Lu	β^-	6.71 d	0.2	133	15
	^{179}Lu	β^-	4.59 h	0.1	464	2
Yttrium	^{90}Y	β^-	2.67 d	2.1×10^{-3}	934	—
Iodine	^{131}I	β^-	8.04 d	2.0	182	10

p/e value is total photon energy emitted per decay divided by total electron energy emitted per decay. Mean electron energy is mean energy of Auger and conversion electrons emitted per decay. Corresponding data for ^{90}Y and ^{131}I are given for comparison.

(1 ng), to a tumor with a radius of 29 mm (100 g). The activity distribution was assumed to be uniform, both in the ellipsoid and in the spheres. The mean absorbed dose rates to the tumor and whole body were calculated. The $TN\dot{D}$ was calculated according to

$$TN\dot{D} = \frac{(\mathrm{TNC}(t) - 1)\left(\sum_i E_{e,i} n_{e,i} \phi_{T,e,i} + \sum_i E_{p,i} n_{p,i} \phi_{T,p,i}\right) + \sum_i E_{e,i} n_{e,i} \phi_{N,e,i} + \sum_i E_{p,i} n_{p,i} \phi_{N,p,i}}{\sum_i E_{e,i} n_{e,i} \phi_{N,e,i} + \sum_i E_{p,i} n_{p,i} \phi_{N,p,i} + \mathrm{TNC}(t) \frac{m_T}{m_N} \sum_i E_{p,i} n_{p,i} (\phi_{N,p,i} - \phi_{T,p,i})}, \quad \text{Eq. 2}$$

where TNC is the tumor-to-normal-tissue activity concentration ratio (*11*), that is, the activity concentration in the tumor divided by the activity concentration in the normal tissue. $E_{e,i}$ and $E_{p,i}$ are the energies of the emitted electrons and photons, respectively, per transition i; $n_{e,i}$ and $n_{p,i}$ are the numbers of emitted electrons and photons, respectively, per decay; $\phi_{T,e,i}$, $\phi_{T,p,i}$, $\phi_{N,e,i}$, and $\phi_{N,p,i}$ are the absorbed fractions of electrons and photons in tumor and normal tissue, respectively; and m_T and m_N are the masses of the tumor and normal tissue, respectively. The absorbed fractions of electrons and positrons were calculated using Berger's point kernel data (*19*). The absorbed fractions for photons were taken from MIRD pamphlets 3 (*20*) and 8 (*21*). The decay data were taken from the *Table of Radioactive Isotopes* (*22,23*). The electrons emitted in the normal tissue were assumed to be locally absorbed, and thus $\phi_{N,e,i}$ was set at 1.

The dependence of the TNC value on the $TN\dot{D}$ values was calculated for the radiolanthanide ^{177}Lu. $TN\dot{D}$ values were calculated for TNC values ranging from 2 to 100. The further calculations used a TNC value of 25; that is, the activity concentration was assumed to be 25 times higher in the tumor than in normal tissue.

RESULTS

The dependence of the TNC value on the $TN\dot{D}$ values of ^{177}Lu can be seen in Figure 1. The maximum possible $TN\dot{D}$ value is equal to the TNC value; therefore, the results are shown as the $TN\dot{D}$ values divided by the TNC values. The shapes of the $TN\dot{D}$/TNC values as a function of tumor size will be similar for TNC values over 5. The $TN\dot{D}$ values

TABLE 2
Decay Data for the Positron Emitters Studied (*22,23*)

Element	Radionuclide	Decay mode	Half-life	Positron yield	p/e	Total p/e	Mean electron energy (keV/decay)	Mean positron energy (keV/decay]
Cerium/lanthanum	^{134}Ce/^{134}La	EC/EC, β^+	3.16 d/6.45 min	0.63	4.4/0.95	0.98	6/2	−/756
Neodymium/ praseodymium	^{140}Nd/^{140}Pr	EC/EC, β^+	3.37 d/3.39 min	0.51	4.78/1.00	1.04	6/4	−/544
Neodymium	^{141}Nd	EC, β^+	2.49 h	0.025	5.05	5.05	6	9

p/e value is total photon energy emitted per decay divided by total electron energy emitted per decay. Total p/e ratio is total photon energy emitted per decay divided by sum of total energy emitted by electrons and positrons per decay. Annihilation photons are included in total photon energy emitted per decay. Mean electron energy is mean energy of Auger and conversion electrons emitted per decay.

divided by the TNC values differ mainly for small tumors (<10 μg).

The $TN\dot{D}$ values as a function of tumor size for the electron-emitting radiolanthanides studied are shown in Figure 2. The $TN\dot{D}$ values increase with tumor size for all radionuclides because of the increase of the specific absorbed fraction in the tumor. Energy absorbed in the normal tissue will not be affected to the same extent when the size of the tumor is increased. Compared with ^{90}Y and ^{131}I—the reference nuclides used—many radiolanthanides had higher $TN\dot{D}$ values for both smaller and larger tumors. The radiolanthanides that showed the highest $TN\dot{D}$ values were ^{153}Sm, ^{161}Tb, ^{169}Er, ^{175}Yb, and ^{177}Lu. ^{169}Er displayed higher $TN\dot{D}$ values than did ^{177}Lu for all tumor sizes studied and the highest $TN\dot{D}$ values of all radiolanthanides studied for tumors larger than 10 μg. The $TN\dot{D}$ values as a function of tumor size were similar for ^{177}Lu, ^{175}Yb, and ^{161}Tb, with somewhat higher $TN\dot{D}$ values for the latter for tumors smaller than 100 μg. For very small tumors (<10 μg), ^{161}Ho displayed the highest $TN\dot{D}$ values of all electron-emitting radiolanthanides studied, whereas for tumors larger than 1 mg, ^{161}Ho had rather low $TN\dot{D}$ values.

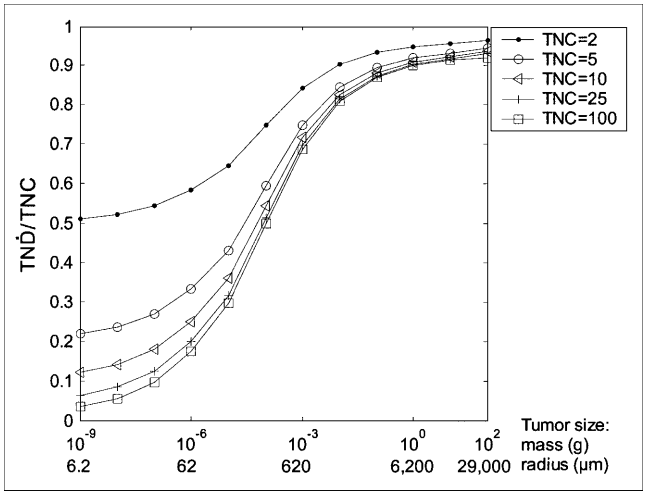

FIGURE 1. $TN\dot{D}$ divided by TNC as function of tumor size for electron-emitting radiolanthanide ^{177}Lu.

^{142}Pr, ^{145}Pr, and ^{166}Ho had $TN\dot{D}$ values similar to those of ^{90}Y. The $TN\dot{D}$ values of ^{143}Pr, ^{149}Pm, ^{150}Eu, ^{159}Gd, ^{165}Dy, ^{176m}Lu, and ^{179}Lu were higher than those of ^{90}Y for all tumor sizes studied.

The electron-emitting radiolanthanides with the highest p/e ratios (>1.8), namely ^{140}La, ^{142}La, ^{150}Pm, ^{156}Eu, and ^{157}Eu, emit medium- and high-energy electrons (>350 keV), leading to low $TN\dot{D}$ values for all tumor sizes studied. ^{172}Tm and ^{173}Tm have electron energies similar to those of ^{140}La, ^{156}Eu, and ^{157}Eu, but the 2 radionuclides of thulium have higher $TN\dot{D}$ values than the 3 other radiolanthanides mentioned, because of their lower p/e ratios (0.9 and 1.3, respectively). ^{167}Ho and ^{167}Tm have high p/e ratios (>1.2) and low electron energies (<200 keV), and the $TN\dot{D}$ values for larger tumors are low.

The $TN\dot{D}$ values as a function of tumor size for the positron-emitting radiolanthanides studied are presented in Figure 3. In general, all positron emitters had low $TN\dot{D}$ values, although ^{141}Nd had relatively high $TN\dot{D}$ values for small tumors.

Routine clinical application requires the availability of radionuclides both at sufficient radioactivities and at high specific activities. ^{177}Lu can be produced in *ca* form by direct neutron activation of ^{176}Lu, with a high cross section (~2,100 b), or in *nca* form via indirect production from β-decay of reactor-produced ^{177}Yb (*24,25*). In theory, it should be possible to produce ^{177}Lu with a specific activity of around 4.1 TBq/mg, according to

$$A = \lambda \cdot N, \qquad \text{Eq. 3}$$

where λ is the decay constant and N is the number of atoms in 1 mg.

^{153}Sm can be produced by neutron bombardment of ^{152}Sm at a rather high specific activity of up to 144 GBq/mg (*26–28*), because of the high cross section (206 b) of the thermal neutron capture reaction. Because this is an (n,γ) reaction, ^{153}Sm will be obtained in the *ca* form.

^{161}Tb can be produced after neutron capture of ^{160}Gd according to ^{160}Gd(n,γ) ^{161}Gd (half-life, 3.6 min) → β^- → ^{161}Tb (*29*). ^{161}Tb subsequently needs to be chemically

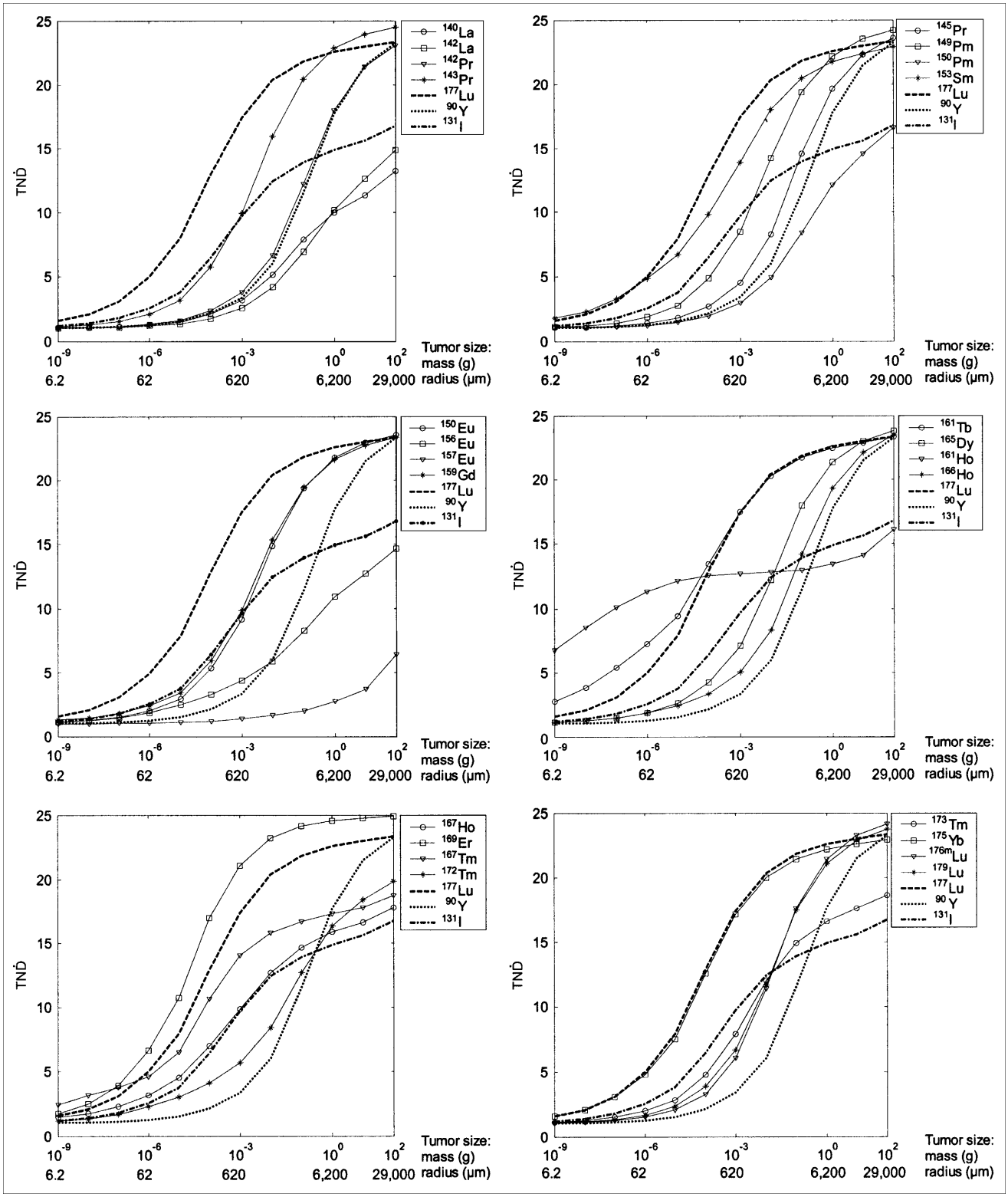

FIGURE 2. *TNḊ* as function of tumor size for electron-emitting radiolanthanides. In all panels, ^{177}Lu, ^{90}Y, and ^{131}I are shown for comparison.

separated from the neighboring gadolinium (*29*). Via this route, ^{161}Tb is in principle obtained in an *nca* form with a theoretic specific activity of 4.3 GBq/mg, according to Equation 3. No direct route is available, and double neutron capture by ^{159}Tb would be the only alternative, providing a rather low specific activity.

^{169}Er was the radiolanthanide with the highest *TNḊ* values for most of the tumors sizes studied. ^{169}Er can be

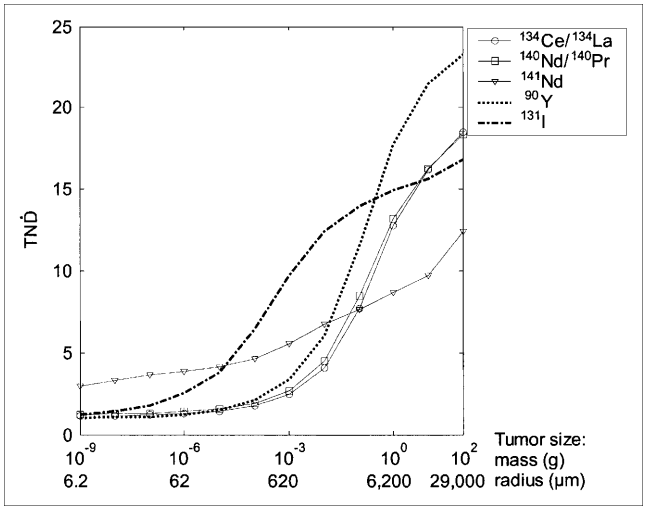

FIGURE 3. *TNḊ* as function of tumor size for positron-emitting radiolanthanides. Corresponding values for ^{90}Y and ^{131}I are shown for comparison.

produced through neutron capture of stable ^{168}Er by the reaction ^{168}Er(n,γ)^{169}Er. However, as the neutron capture cross section of this process is rather low (2 b), the specific activity of the ^{169}Er produced will be low and the nuclide will be obtained in the *ca* form.

^{175}Yb can be produced by thermal neutron bombardment of ytterbium targets isotopically enriched with ^{174}Yb, that is, by the reaction ^{174}Yb(n,γ)^{175}Yb. In contrast to ^{169}Er, the specific activities of ^{175}Yb are high because of the neutron capture cross section of this process (100 b), but ^{175}Yb will still be obtained in a *ca* form.

^{161}Ho is available at particle accelerators, including medical-type cyclotrons. One route is the α-irradiation of ^{159}Tb, or the ^{159}Tb(α,2n)^{161}Ho route. The other route is the irradiation of dysprosium targets using protons or deuterons: ^{161}Dy(p,n), ^{162}Dy(d,2n), or ^{160}Dy(d,n), for example. In theory, ^{161}Ho can be produced with a specific activity of 290 TBq/mg, according to Equation 3. After radiochemical separation, ^{161}Ho is obtained *nca*.

The only radiolanthanide of ^{143}Pr, ^{149}Pm, ^{150}Eu, ^{159}Gd, ^{165}Dy, ^{176m}Lu, and ^{179}Lu that can be produced at high specific activities and *nca* is ^{149}Pm. ^{149}Pm can be produced by the indirect route ^{148}Nd(n,γ)^{149}Nd → ^{149}Pm (*30*). With this method, it would be possible to obtain theoretic specific activities of 15 GBq/mg, according to Equation 3.

^{142}Pr and ^{165}Dy are available in *ca* form only, and production rates of *nca* ^{145}Pr may be too low for routine (and commercial) applications. Thus, *nca* ^{166}Ho available from a ^{166}Dy/^{166}Ho generator, rather than via the ^{165}Ho(n,γ)^{166}Ho process, might be an option for dedicated applications in radionuclide therapy. With the generator, a theoretic specific activity of 26 TBq/mg can be achieved, according to Equation 3.

DISCUSSION

The *TNḊ* model is an analytic method that is easy to use. In this study, a constant TNC and a uniform activity distribution in both the tumor and normal tissue were assumed. The *TNḊ* model is a convenient method for estimating the ratio between the absorbed dose rates to tumors of different sizes and to normal tissue. In this study, the normal tissue was assumed to be the whole body. The bone marrow is usually one of the dose-limiting organs in radionuclide therapy. Absorbed dose to the bone marrow is difficult to estimate, but bone marrow toxicity correlates, in some applications, with absorbed dose to the whole body (*31*). Whether the same is true for other clinical situations remains to be studied.

It is possible to determine the ratio between the absorbed dose to the tumor and normal tissue, TND, by adding biokinetic data in the form of changes in the TNC and taking the half-lives of the radionuclides into consideration. Because the TNC varies considerably between different substances and tissues and also with time, such calculations are needed for a detailed evaluation of the usefulness of interesting radionuclides bound to a specific radiopharmaceutical. We chose to perform the calculations for a constant TNC value of 25. This choice was based on the assumption that a large tumor would need an absorbed dose of 100 Gy to be sterilized, whereas normal tissue, such as bone marrow, could endure an absorbed dose of 4 Gy. However, Figure 1 shows that the shape of the *TNḊ*/TNC values as a function of tumor size will not vary significantly for TNC values higher than about 5. Therefore, using another TNC value will yield results and conclusions similar to those obtained in this study. The results are not prejudiced by any biokinetics, and they can be used as a guide for further studies on a defined pharmaceutical and tumor model. Especially, our results demonstrate radiolanthanides not suitable for therapy of patients because of the high contribution of photons, irrespective of the radiopharmaceutical used.

A large abundance of photons will reduce the therapeutic potential of the radionuclide, as is well demonstrated by the *TNḊ* model, which shows decreasing *TNḊ* values with increasing photon emission. The model also gives information about the tumor sizes for which the absorbed fraction of emitted electrons is high. On the basis of the results of the *TNḊ* calculations, the radiolanthanides can be divided into 5 different groups. To the first group belong the low-energy (100−250 keV) electron emitters with low photon abundance (p/e < 0.3) and high *TNḊ* values even for rather small tumors: ^{153}Sm, ^{161}Tb, ^{169}Er, ^{175}Yb, and ^{177}Lu. In this group, the only radionuclides that can be produced in sufficient amounts and *nca* are ^{177}Lu and ^{161}Tb. The use of radionuclides in *nca* form and with high specific activities is important when biologically active peptides such as somatostatin analogs are used. In other cases, the use of radionuclides with lower specific activities and in *ca* form might be possible. ^{177}Lu and ^{161}Tb have similar *TNḊ* values and physical half-lives. However, the different emission of Auger electrons will make these 2 radionuclides of special interest in studying the Auger effect for various internalizing

radiopharmaceuticals, such as radiolabeled somatostatin analogs (*32*).

The lower specific activities of ^{153}Sm, ^{169}Er, and ^{175}Yb are quite acceptable for specific therapeutic strategies such as radiosynoviorthesis or palliative treatment of disseminated bone metastases. Additionally, significant batch activities are easily achievable for ^{153}Sm and ^{175}Yb. However, their use for the labeling of tumor receptor– or antigen-targeting vectors might be limited because of the much higher specific activities required.

The second group consists of the Auger-electron emitters ^{161}Ho and ^{167}Tm. These 2 radiolanthanides emit photons in high abundance (p/e $>$ 1.2). ^{161}Ho displays high $TN\dot{D}$ values for small tumors because of its low electron energies (Table 1) but has low $TN\dot{D}$ values for tumors larger than 1 mg (radius, 0.62 mm), because of the significant accompanying photon emission. Also, the low-energy electron emitter ^{161}Tb might be included in this group because of the significant quantity of Auger-electrons emitted. These radiolanthanides emit low-energy β- or conversion electrons that make them especially interesting for radiopharmaceuticals that are internalized by the tumor cells but not by the dose-limiting normal cells. If these nuclides are internalized into the nucleus of the cell, the influence on the absorbed dose to the nucleus from the low-energy electrons will be increased, compared with the absorbed dose from the electrons with higher energies and the photons. In other words, when one is calculating the absorbed dose rate to the cell nucleus, the $TN\dot{D}$ values will increase if the radionuclide is internalized into the tumor cells but not into the normal cells. The short range of Auger electrons might require that labeled compounds approach the cell nucleus subsequent to internalization, in turn requiring new and efficient chemical and radiopharmaceutical targeting strategies. Another problem with low-energy electrons is that all cells must be targeted in order to achieve a uniform distribution of absorbed dose in the tumor. It has been demonstrated theoretically that therapy with radionuclides emitting very-low-energy electrons would be difficult if not all the cells are targeted (*33,34*). ^{161}Ho, ^{167}Tm, and ^{161}Tb might be useful radionuclides for further investigations of the significance of Auger electrons in therapeutic applications. Another radiolanthanide that also demonstrates a relatively high emission of Auger electrons is ^{153}Sm. However, ^{153}Sm can be produced only *ca* and in too low a specific activity.

The third group consists of the medium-energy (280–470 keV) electron emitters with low photon abundance (p/e $<$ 0.2): ^{143}Pr, ^{149}Pm, ^{150}Eu, ^{159}Gd, ^{165}Dy, ^{176m}Lu, and ^{179}Lu. These radiolanthanides have $TN\dot{D}$ values similar to that of ^{131}I for small tumors and even higher $TN\dot{D}$ values for larger tumors, because of their lower photon emission. However, the only radionuclide that can be produced in high specific activities (15 GBq/mg) and *nca* is ^{149}Pm.

The fourth group comprises the high-energy (>650 keV) electron emitters with low photon abundance (p/e $<$ 0.1). These are ^{142}Pr, ^{145}Pr, and ^{166}Ho, of which ^{166}Ho is the only nuclide that can be produced in sufficient amounts. High-energy-electron–emitting radionuclides are suitable for large tumors (>1 g), but the low absorbed electron energy fraction in small tumors might limit their use for treatment of disseminated diseases with small tumor nests (*34,35*). However, nonuniform activity distributions in tumors might necessitate the use of high-energy electron emitters to obtain a uniform absorbed dose (*34*). A greater number of experimental studies are required, and the generator-produced high-energy-electron–emitting ^{166}Ho might be a valuable component of well-designed experimental studies.

The fifth group contains radiolanthanides with a high photon emission (p/e $>$ 0.9).These are ^{140}La, ^{142}La, ^{150}Pm, ^{156}Eu, ^{157}Eu, ^{167}Ho, ^{172}Tm, ^{173}Tm, and the positron-emitting radiolanthanides. Their p/e values result in low $TN\dot{D}$ values for all tumor sizes. Using these radionuclides for therapy will result in a high absorbed dose to the whole body and most probably in bone marrow toxicity. All these radionuclides have higher p/e ratios or higher mean electron energy and lower $TN\dot{D}$ values than does ^{131}I (p/e = 2, E = 182 keV). Therefore, in searches for more optimal radionuclides, one criterion should be a p/e ratio lower than that of ^{131}I (*12*).

In this study, we identified a total of 6 radiolanthanides that might be suitable for binding to tumor-seeking pharmaceuticals, namely ^{149}Pm, ^{161}Tb, ^{161}Ho, ^{166}Ho, ^{167}Tm, and ^{177}Lu. Five of these radionuclides have half-lives of between 1.1 and 9.2 d, whereas ^{161}Ho has a half-life of only 2.5 h. This short half-life might limit the use of this radionuclide for systemic therapies, but it might be suitable for local therapies, such as intratumoral therapy of brain tumors. The 6 selected radiolanthanides include electron emitters within the low-energy (E $<$ 250 keV), medium-energy (280−470 keV), and high-energy (>650 keV) regions.

CONCLUSION

Six radiolanthanides that might be suitable for radionuclide therapy were selected, among them the low-energy electron emitters ^{177}Lu, ^{161}Tb, ^{167}Tm, and ^{161}Ho. Because production routes are available to obtain ^{161}Tb and ^{177}Lu routinely in *nca* form, these radionuclides might be interesting choices for dedicated radionuclide therapeutic applications. ^{161}Ho, with its short half-life, might be suitable for local radionuclide therapy. If radionuclides emitting higher electron energies are needed, the medium-energy electron emitter ^{149}Pm and the high-energy electron emitter ^{166}Ho may, in principle, be used instead of ^{90}Y.

ACKNOWLEDGMENTS

This study was supported by the Swedish Cancer Society (grants 3427 and 4956) and the King Gustav V Jubilee Clinic Foundation, Sweden, and was carried out within the European Cooperation in the Field of Science and Technology programs COST D18 and COST B12.

REFERENCES

1. Rösch F, Forssell-Aronsson E. Radio-lanthanides in nuclear medicine. In: Sigel H, ed. *Metal Ions and Their Complexes in Medication.* New York, NY: Marcel Dekker, Inc.; 2004:77–108.
2. Schmitt A, Bernhardt P, Nilsson O, et al. Radiation therapy of small cell lung cancer with ^{177}Lu-DOTA-Tyr^3-octreotate in an animal model. *J Nucl Med.* 2004;45:1542–1548.
3. de Jong M, Breeman WA, Bernard BF, et al. [^{177}Lu-DOTA^0,Tyr^3]octreotate for somatostatin receptor-targeted radionuclide therapy. *Int J Cancer.* 2001;92: 628–633.
4. Koppe MJ, Bleichrodt RP, Soede AC, et al. Biodistribution and therapeutic efficacy of $^{125/131}$I, ^{186}Re-, $^{88/90}$Y-, or ^{177}Lu-labeled monoclonal antibody MN-14 to carcinoembryonic antigen in mice with small peritoneal metastases of colorectal origin. *J Nucl Med.* 2004;45:1224–1232.
5. Kwekkeboom DJ, Bakker WH, Kooij PP, et al. [^{177}Lu-DOTA^{0}Tyr^3]octreotate: comparison with [^{111}In-DTPA^0]octreotide in patients. *Eur J Nucl Med.* 2001;28: 1319–1325.
6. Kwekkeboom DJ, Bakker WH, Kam BL, et al. Treatment of patients with gastro-entero-pancreatic (GEP) tumours with the novel radiolabelled somatostatin analogue [^{177}Lu-DOTA^0,Tyr^3]octreotate. *Eur J Nucl Med Mol Imaging.* 2003; 30:417–422.
7. Kwekkeboom DJ, Teunissen JJ, Bakker WH, et al. Radiolabeled somatostatin analog [^{177}Lu-DOTA^0,Tyr^3]octreotate in patients with endocrine gastroenteropancreatic tumors. *J Clin Oncol.* 2005;23:2754–2762.
8. Teunissen JJ, Kwekkeboom DJ, Krenning EP. Quality of life in patients with gastroenteropancreatic tumors treated with [^{177}Lu-DOTA^0,Tyr^3]octreotate. *J Clin Oncol.* 2004;22:2724–2729.
9. Forrer F, Uusijärvi H, Storch D, Maecke H, Mueller-Brand J. Treatment with ^{177}Lu-DOTATOC of patients with relapse of neuroendocrine tumors after treatment with ^{90}Y-DOTATOC. *J Nucl Med* 2005;46:1310–1316.
10. Wessels BW, Rogus RD. Radionuclide selection and model absorbed dose calculations for radiolabeled tumor associated antibodies. *Med Phys.* 1984;11: 638–645.
11. Bernhardt P, Benjegard SA, Kolby L, et al. Dosimetric comparison of radionuclides for therapy of somatostatin receptor-expressing tumors. *Int J Radiat Oncol Biol Phys.* 2001;51:514–524.
12. Bernhardt P, Forssell-Aronsson E, Jacobsson L, Skarnemark G. Low-energy electron emitters for targeted radiotherapy of small tumours. *Acta Oncol.* 2001;40: 602–608.
13. Mäcke H, Good S. Radiometals (non-Tc, non-Re) and bifunctional labeling chemistry. In: Vèrtes A, Nagy S, Klencsár Z, Rösch F, eds. *Handbook of Nuclear Chemistry, Volume 4.* Dordrecht, The Netherlands: Kluwer Academic Publishers; 2003:279–314.
14. Breeman WA, de Jong M, de Blois E, Bernard BF, Konijnenberg M, Krenning EP. Radiolabelling DOTA-peptides with ^{68}Ga. *Eur J Nucl Med Mol Imaging.* 2005;32:478–485.
15. Mirzadeh S, Mauser LF, Garland MA. Reactor-produced medical radionuclides. In: Vèrtes A, Nagy S, Klencsár Z, Rösch F, eds. *Handbook of Nuclear Chemistry, Volume 4.* Dordrecht, The Netherlands: Kluwer Academic Publishers; 2003: 1–46.
16. Rösch F, Knapp F. Radionuclide generators. In: Vèrtes A, Nagy S, Klencsár Z, Rösch F, eds. *Handbook of Nuclear Chemistry, Volume 4.* Dordrecht, The Netherlands: Kluwer Academic Publishers; 2003:81–118.
17. Rösch F, Brockmann J, Lebedev NA, Qaim SM. Production and radiochemical separation of the Auger electron emitter ^{140}Nd. *Acta Oncol.* 2000;39:727–730.
18. Lubberink M, Lundqvist H, Tolmachev V. Production, PET performance and dosimetric considerations of ^{134}Ce/^{134}La, an Auger electron and positron-emitting generator for radionuclide therapy. *Phys Med Biol.* 2002;47:615–629.
19. Berger MJ. *Improved Point Kernel for Electrons and Beta-Ray Dosimetry.* Washington DC: U.S. Atomic Energy Commission; 1973.
20. Brownell GL, Ellett WH, Reddy AR. Absorbed fractions for photon dosimetry. *J Nucl Med.* 1968;(suppl 1):27–39.
21. Ellett W, Humes R. Absorbed fractions for small volumes containing photon-emitting radioactivity. *J Nucl Med.* 1972;13(suppl 5):26–32.
22. Browne E, Firestone RB. *Table of Radioactive Isotopes.* New York, NY: Wiley–Interscience Publication; 1986.
23. Chu SYF, Ekström LP, Firestone RB. WWW Table of Radioactive Isotopes. 1999. Available at: http://nucleardata.nuclear.lu.se/nucleardata/toi/. Accessed March 20, 2006.
24. Lebedev NA, Novgorodov AF, Misiak R, Brockmann J, Rosch F. Radiochemical separation of no-carrier-added ^{177}Lu as produced via the ^{176}Yb(n,gamma)^{177}Yb→ ^{177}Lu process. *Appl Radiat Isot.* 2000;53:421–425.
25. Cutler CS, Ehrhardt GJ, Tyler TT, Jurisson SS, Deutsch E. Current and potential therapeutic uses of lanthanide radioisotopes. *Cancer Biother Radiopharm.* 2000; 15:531–545.
26. Ramamoorthy N, Saraswathy P, Das MK, Mehra KS, Ananthakrishnan M. Production logistics and radionuclidic purity aspects of ^{153}Sm for radionuclide therapy. *Nucl Med Commun.* 2002;23:83–89.
27. Neves M, Kling A, Lambrecht RM. Radionuclide production for therapeutic radiopharmaceuticals. *Appl Radiat Isot.* 2002;57:657–664.
28. Tse JW, Wiebe LI, Noujaim AA. High specific activity [samarium-153] EDTA for imaging of experimental tumor models. *J Nucl Med.* 1989;30:202–208.
29. de Jong M, Breeman WA, Bernard BF, et al. Evaluation in vitro and in rats of ^{161}Tb-DTPA-octreotide, a somatostatin analogue with potential for intraoperative scanning and radiotherapy. *Eur J Nucl Med.* 1995;22:608–616.
30. Hu F, Cutler CS, Hoffman T, Sieckman G, Volkert WA, Jurisson SS. Pm-149 DOTA bombesin analogs for potential radiotherapy: in vivo comparison with Sm-153 and Lu-177 labeled DO3A-amide-betaAla-BBN(7-14)NH(2). *Nucl Med Biol.* 2002;29:423–430.
31. Wahl RL, Kroll S, Zasadny KR. Patient-specific whole-body dosimetry: principles and a simplified method for clinical implementation. *J Nucl Med.* 1998; 39(suppl):14S–20S.
32. Andersson P, Forssell-Aronsson E, Johanson V, et al. Internalization of indium-111 into human neuroendocrine tumor cells after incubation with indium-111-DTPA-D-Phe1-octreotide. *J Nucl Med.* 1996;37:2002–2006.
33. Bernhardt P, Ahlman H, Forssell-Aronsson E. Model of metastatic growth valuable for radionuclide therapy. *Med Phys.* 2003;30:3227–3232.
34. O'Donoghue JA. Implications of nonuniform tumor doses for radioimmunotherapy. *J Nucl Med.* 1999;40:1337–1341.
35. Bernhardt P, Ahlman H, Forssell-Aronsson E. Modelling of metastatic cure after radionuclide therapy: influence of tumor distribution, cross-irradiation, and variable activity concentration. *Med Phys.* 2004;31:2628–2635.